Magnetic and Structural Studies of Copper–Lanthanoid Complexes; the Synthesis and Structures of New Cu_3Ln Complexes of 6-Chloro-2-pyridone ($Ln = Gd$, Dy and Er) and Magnetic Studies on Cu_2Gd_2, Cu_4Gd_2 and Cu_3Gd Complexes

Cristiano Benelli,* Alexander J. Blake, Paul E. Y. Milne, Jeremy M. Rawson and Richard E. P. Winpenny*

Abstract: The synthesis and structural characterisation of three copper–lanthanoid complexes are reported. The compounds, of general formula $[Cu_3M(chp)_8(NO_3)(S)]$ [$M = Gd$, $S = H_2O$ in **2**; $M = Dy$, $S = H_2O$ in **3**; $M = Er$, $S = (H_2O)_{0.5}(MeOH)_{0.5}$ in **4**; chp = anion of 6-chloro-2-pyridone], are made by reaction of $[Cu_2(chp)_4]$ (**1**) with the hydrated lanthanoid nitrate salt in methanol. Structural studies reveal the three copper atoms lie in an approximate hemisphere about a central lanthanoid atom. Magnetic studies on **2** and two further Cu–Gd complexes show ferromagnetic coupling between the 3d and 4f metals. Consideration of these results along with magnetic data previously reported for Cu–Gd compounds leads to a correlation between the magnitude of this exchange coupling and the exponential of the Cu···Gd distance. This is the first magneto–structural correlation reported for mixed d-block/f-block metal complexes.

Keywords: copper compounds · exchange coupling · heterometallic compounds · lanthanide compounds · magnetic properties · structure elucidation

Introduction

Direct ferromagnetic coupling between copper(II) and gadolinium(III) was first reported in 1985,[1] and since that time a number of research groups have begun to explore the magnetic properties of molecules that contain both d- and f-block metals.[2–7] The molecules have featured polydentate Schiff-base ligands[1–3] encapsulating both metals and 2-propylene-bis(oximato) ligands[5] or pyridone ligands[4,7] bridging the metals. We have recently reported a number of polynuclear mixed copper–lanthanoid complexes[4,8–11] containing derivatives of 2-pyridone as a ligand. As these compounds exhibit a range of Cu-to-Ln ratios, a diversity of bridging motifs and a range of Cu···Ln distances within the molecules, we have investigated the magnetic exchange interactions in three of these compounds, hoping to find some correlation between the magnitude of the exchange coupling and some structural feature.

Results

Synthesis and Structures: We have previously reported[10] the reaction of $[Cu_2(chp)_4]$ (**1**) (chp = anion of 6-chloro-2-pyridone) with hydrated lanthanum nitrate in methanol, which gave the complex $[Cu_3La(chp)_5(NO_3)_3(OMe)(MeOH)_2]$. The same reaction with gadolinium, dysprosium or erbium in place of lanthanum led to a different product, namely, $[Cu_3M(chp)_8(NO_3)(S)]$ [$M = Gd$, $S = H_2O$ in **2**; $M = Dy$, $S = H_2O$ in **3**; $M = Er$, $S = (H_2O)_{0.5}(MeOH)_{0.5}$ in **4**]. These complexes strongly resemble the product obtained from reaction of $[La(NO_3)_3]\cdot 5H_2O$ with **1** in ethanol.[10]

Complexes **2**, **3** and **4** were obtained as dark green crystalline materials by diffusion of ether vapour into a methanolic solution. X-ray structural analysis, details of which are given in Table 1, revealed in each case a complex in which three chemically distinct copper atoms are found in a semicircular array surrounding the f-block atom (Fig. 1). The first copper is bound to two N and two O atoms from chp ligands, with a *cis* geometry for these donor atoms. The second is bound to one O and two N atoms from chp units; the final coordination site is occupied by one molecule of solvent, which for **2** and **3** is water but for **4** is half-occupied by water and half by methanol. The third copper atom is bound to three nitrogens and one oxygen from chp ligands. All copper coordination spheres are based on square-planar geometries, but considerably distorted therefrom. Selected bond lengths and angles for **2** are given in Tables 2 and 3; due to the lanthanoid contraction, bond lengths for **3** and **4** are slightly shorter than equivalent bonds in **2**; bond angles are very similar in the three structures.

The lanthanoid atoms are eight-coordinate, bound to two μ-oxygens from trinucleating chp ligands shared with Cu1, four further O atoms from mono- or binucleating chp moieties and two O atoms from a bidentate nitrate ion. Although the geometry is based on a bicapped trigonal prism, the distortion from this geometry is considerable. As we have found previously in

---

[*] Prof. C. Benelli
Department of Chemistry, University of Florence
Via Maragliano 77, 50144 Florence (Italy)

Dr R. E. P. Winpenny, Dr. A. J. Blake, Dr. P. E. Y. Milne, Dr. J. M. Rawson
Department of Chemistry, The University of Edinburgh
West Mains Road, Edinburgh EH9 3JJ (UK)
Telefax: Int. code + (131) 650-4743

0947-6539/95/0109-0614 $ 10.00+.25/0

Table 1. Experimental data for the X-ray studies of compounds **2**, **3** and **4**.

Compound	**2**	**3**	**4**
formula	$C_{40}H_{26}Cl_8Cu_3GdN_9O_{12}\cdot 0.5CH_3OH$	$C_{40}H_{26}Cl_8Cu_3DyN_9O_{12}\cdot CH_3OH$	$C_{41}H_{28}Cl_8Cu_3ErN_9O_{12}\cdot CH_3OH$
formula weight	1470	1493	1512
a/Å	10.744(6)	10.741(7)	10.797(7)
b/Å	12.131(7)	12.136(7)	12.104(8)
c/Å	21.138(18)	21.199(14)	21.286(11)
α/°	78.48(3)	78.02(6)	77.74(4)
β/°	78.06(5)	78.01(3)	78.10(3)
γ/°	77.30(3)	77.40(4)	77.67(4)
U/Å^3	2602	2600	2618
ρ_{calcd}/gcm^{-1}	1.88	1.91	1.92
crystal size/mm	0.39 × 0.27 × 0.12	0.35 × 0.14 × 0.05	0.39 × 0.23 × 0.03
μ/mm^{-1}	2.97	3.13	3.30
unique data [$5 \leq 2\theta \leq 45°$]	6847	6925	5704
observed data [$I > 2\sigma(I)$]	5372	4587	4178
no. of refined parameters	667	675	370
max. Δ/σ ratio	0.032	0.001	0.044
R, R' [a]	0.0320, 0.0342	0.0560, 0.0685	0.0449, 0.0407
weighting scheme, w^{-1}	$\sigma^2(F) + 0.000285\,F^2$	$\sigma^2(F) + 0.000461\,F^2$	$\sigma^2(F) + 0.000059\,F^2$
largest residuals/eÅ^{-3}	+1.31	+1.58	+1.12

[a] SHELX-76 [18]: Common features: crystal system, triclinic; space group, $P\bar{1}$; $Z = 2$; $T = 150.0(2)$ K; radiation, $Mo_{K\alpha}$; dark green plate.

Table 2. Selected bond lengths (Å) for compound **2**.

Gd1–O1r	2.270(4)	Cu1–N6r	1.997(5)
Gd1–O3r	2.462(4)	Cu1–O7r	1.959(4)
Gd1–O4r	2.296(4)	Cu2–N1r	1.972(5)
Gd1–O5r	2.239(4)	Cu2–O2r	1.939(4)
Gd1–O7r	2.484(4)	Cu2–N7r	1.999(5)
Gd1–O8r	2.297(4)	Cu2–O1w	1.955(5)
Gd1–O11n	2.528(5)	Cu3–N3r	2.007(5)
Gd1–O21n	2.510(5)	Cu3–N4r	2.018(5)
Cu1–N2r	1.971(5)	Cu3–O6r	1.965(4)
Cu1–O3r	1.956(4)	Cu3–N8r	1.987(5)

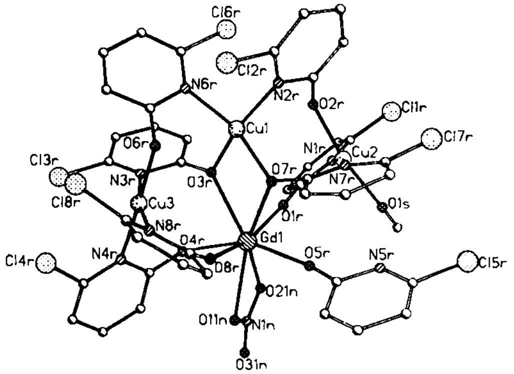

Fig. 1. The structure of **2** in the crystal showing the crystallographic numbering scheme. Complexes **3** and **4** are essentially isostructural, differing only in the lanthanoid atom involved, and in the solvent molecule attached to Cu 2 (see text).

Table 3. Selected bond angles (°) for compound **2**.

O1r-Gd1-O3r	75.71(15)	O7r-Gd1-O11n	143.70(14)
O1r-Gd1-O4r	105.74(15)	O7r-Gd1-O21n	149.61(14)
O1r-Gd1-O5r	90.53(16)	O8r-Gd1-O11n	75.70(14)
O1r-Gd1-O7r	83.95(15)	O8r-Gd1-O21n	126.29(15)
O1r-Gd1-O8r	161.03(15)	O11N-Gd1-O21n	50.80(15)
O1r-Gd1-O11n	123.10(15)	N2r-Cu1-O3r	160.34(19)
O1r-Gd1-O21n	72.68(15)	N2r-Cu1-N6r	95.81(20)
O3r-Gd1-O4r	70.95(14)	N2r-Cu1-O7r	96.01(19)
O3r-Gd1-O5r	136.75(15)	O3r-Cu1-N6r	93.24(19)
O3r-Gd1-O7r	61.20(13)	O3r-Cu1-O7r	80.06(17)
O3r-Gd1-O8r	90.29(14)	N6r-Cu1-O7r	161.57(19)
O3r-Gd1-O11n	142.50(14)	N1r-Cu2-O2r	88.28(20)
O3r-Gd1-O21n	127.78(14)	N1r-Cu2-N7r	170.46(21)
O4r-Gd1-O5r	151.59(15)	N1r-Cu2-O1w	91.04(21)
O4r-Gd1-O7r	127.04(14)	O2r-Cu2-N7r	92.74(19)
O4r-Gd1-O8r	80.98(14)	O2r-Cu2-O1w	170.32(20)
O4r-Gd1-O11n	72.60(14)	N7r-Cu2-O1w	89.54(21)
O4r-Gd1-O21n	79.01(14)	N3r-Cu3-N4r	91.35(20)
O5r-Gd1-O7r	76.88(15)	N3r-Cu3-O6r	88.24(18)
O5r-Gd1-O8r	91.11(15)	N3r-Cu3-N8r	168.31(20)
O5r-Gd1-O11n	78.90(15)	N4r-Cu3-O6r	178.51(19)
O5r-Gd1-O21n	84.05(15)	N4r-Cu3-N8r	97.06(20)
O7r-Gd1-O8r	78.04(14)	O6r-Cu3-N8r	83.55(19)

these systems,[9–11] and has been frequently shown by others,[12] the lanthanoid–oxygen bond lengths depend on the source of the oxygen atom; in this case the shortest bonds are to the four O atoms from binucleating chp ligands; those involving the μ_2-oxygens are slightly longer, and longer yet are those to the nitrate oxygen atoms.

Magnetic Studies: Our recent synthetic work has led to several different structures, each containing both copper and a lanthanoid. For gadolinium, which is the simplest paramagnetic lanthanoid to study as orbital contributions to the magnetism of this ion are negligible, three of these structural types are known: **2**, **5**[4] and **6**[11] (hp = 2-hydroxypyridine, mhp = 6-methyl-2-pyridone. Each contains a different ratio of Cu to Gd, and also

$[Cu_3Gd(chp)_8(NO_3)(H_2O)]$ **2**

$[Cu_4Gd_2(hp)_8Cl_4(Hhp)_4(H_2O)_4]\cdot 2Cl\cdot H_2O$ **5**

$[Cu_2Gd_2(mhp)_4(OMe)_2(NO_3)_4(Hmhp)_2(MeOH)_2]$ **6**

different spatial arrangements of the metals. Figure 2 is a schematic representation showing these arrangements and the bridging atoms.

In **2** the four metals present are arranged in an approximately planar quadrilateral. The shortest contact is that between Cu 1 and Gd 1 (3.60 Å), which is bridged by two μ-O atoms, while the Cu ⋯ Cu contacts are between 3.61 and 3.70 Å. A distorted octahedron of metals is observed in **5**, with Gd atoms in axial positions and four Cu atoms in an equatorial region. Two of the Gd ⋯ Cu contacts are approximately 3.56 Å; the other two are much longer. All the Cu ⋯ Cu contacts around the edge of the

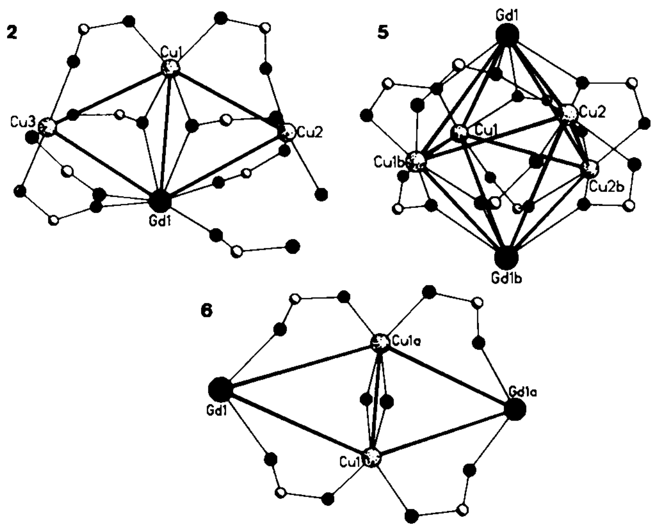

Fig. 2. A schematic representation showing the Cu–Cu and Cu–Gd contacts in complexes **2**, **5** and **6**. M–M contacts shown as thick lines; atoms involved in bridging metals shown linked with thin lines. M–M distances [Å] (average esd 0.001 Å) for **2**: Gd1–Cu1 3.627, Gd1–Cu2 3.922, Gd1–Cu3 3.743, Cu1–Cu2 3.688, Cu1–Cu3 3.695, Cu2–Cu3 6.575; for **5** Gd1–Cu1 3.546, Gd1–Cu2 3.549, Gd1–Cu1b 4.334, Gd1–Cu2b 4.331; for **6** Cu1–Cu1a 2.971, Gd1–Cu1 4.287, Gd1–Cu1a 4.283.

equatorial plane are between 3.84 and 3.92 Å. In **6** the structure is again quite different, with the four metals arranged in a rhombus. The shortest contact is the Cu ··· Cu contact of 2.97 Å at the centre of the molecule. The two atoms are bridged by two μ_2-oxygens derived from methoxide ligands. The Cu ··· Gd contacts are long at around 4.28 Å.

For **2** the behaviour of χT as a function of temperature in the range 2–60 K is shown in Figure 3. The room-temperature limit corresponds nicely to the expected value for one Gd^{III} ($S = {}^7/_2$) and three Cu^{II} ($S = {}^1/_2$) uncoupled species ($\chi T_{calcd} = 9.0$, $\chi T_{obs} = 9.06$ emu K mol^{-1}). The χT curve shows a maximum of 9.28 emu K mol^{-1} at 22.6 K followed by a decrease to 8.70 emu K mol^{-1} at 2.71 K.

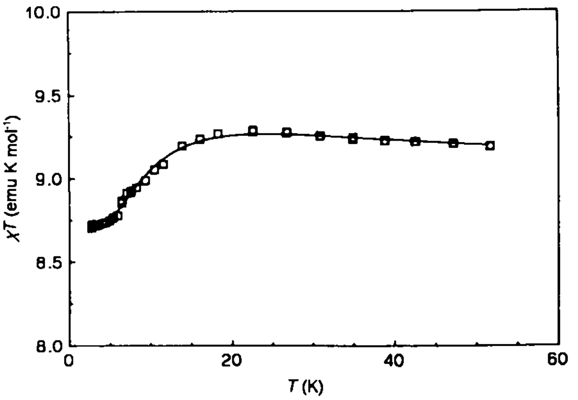

Fig. 3. A plot of χT against T for **2**. Experimental data are shown as squares; best theoretical fit is shown as a full line.

The temperature dependence of χT for **5** is shown in Figure 4. Again the high-temperature limit compares nicely with the expected value for noninteracting spins (χT_{calcd} for two $S = {}^7/_2$ spins and four $S = {}^1/_2$ spins $= 17.25$, $\chi T_{obs} = 17.45$ emu K mol^{-1}). A maximum value of 18.21 emu K mol^{-1} is observed at 38.4 K, while at the lowest temperature limit (4.63 K) the value is 10.11 emu K mol^{-1}.

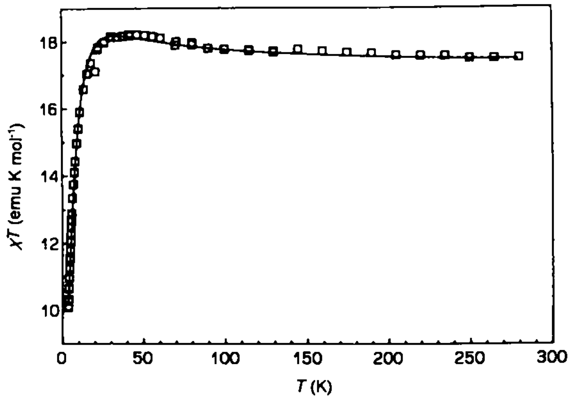

Fig. 4. A plot of χT against T for **5**. Experimental data are shown as squares; best theoretical fit is shown as a full line.

The temperature dependence of χT for **6** is shown in Figure 5. The high-temperature value corresponds quite well to the expected value for two $S = {}^7/_2$ and two $S = {}^1/_2$ uncoupled species ($\chi T_{calcd} = 16.5$, $\chi T_{obs} = 16.48$ emu K mol^{-1}). With decreasing the temperature, the χT values undergo a slight increase, reaching a maximum value of 16.81 emu K mol^{-1} at 11.3 K: on lowering the temperature further the observed values decrease rapidly to a minimum value of 14.41 emu K mol^{-1} at 2.41 K. The temperature dependence of the magnetic susceptibility of the analogous compound where the paramagnetic Gd^{III} ion is substituted by diamagnetic La^{III} shows a pattern with a maximum at approximately 26 K, then a decrease till 8 K, followed by a sharp increase for lower temperatures.

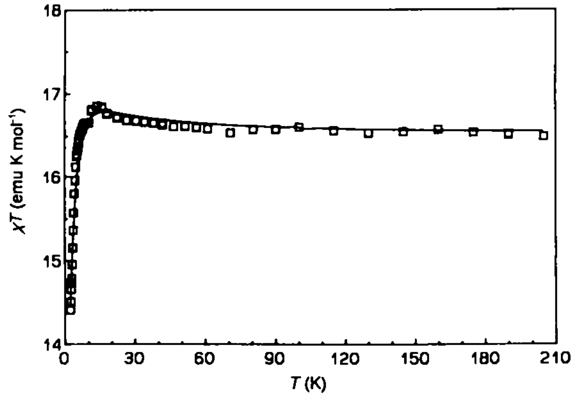

Fig. 5. A plot of χT against T for **6**. Experimental data are shown as squares; best theoretical fit is shown as a full line.

Discussion

The magnetic measurements performed on **2**, **5** and **6** show similar behaviour for all the systems. These data provide some qualitative information on the magnetic structure of these compounds. By comparing these results with previous findings on compounds containing Gd–Cu pairs in magnetic exchange conditions, it is possible to derive the presence of either ferro- or antiferromagnetic interactions.

A ferromagnetic interaction could be at the origin of the maximum observed in all the χT curves, with a value which is above the spin-only limit, while an antiferromagnetic exchange

0947-6539/95/0109-0616 $ 10.00+.25/0

could determine the decrease at low temperature towards values below the spin-only value. All these interactions must be weak, as shown by the high-temperature limits, which are close to the values expected for noninteracting spins.

In order to model these experimental results and to estimate the magnitude of the exchange terms between metals, we have calculated the energy levels, and hence the magnetic susceptibility of the compounds, by means of a technique based on an irreducible tensor method, which has been recently reported.[13] We have used the method developed for high-nuclearity spin clusters even for the simpler systems investigated; this allows more satisfactory comparisons to be made between results obtained on different compounds. The starting point of our calculation was the use of the appropriate Heisenberg spin Hamiltonian, as neither Gd^{III} nor Cu^{II} ions have orbitally degenerate ground states. A specific Hamiltonian was developed for each derivative with a coupling scheme based on the molecular structure observed in the solid state (see Fig. 2).

The simplest system to model is **6**. The magnetic susceptibility of **6** was fitted by using a spin Hamiltonian that includes one Gd–Cu and one Cu–Cu coupling constant as suggested by the structure of the complex, assuming that the extended Cu-N-O-Gd bridges are all equivalent. The fitting procedure, based on a numerical method that extensively uses the MINUIT subroutine,[14] suggested the presence of an antiferromagnetic Cu–Cu and a ferromagnetic Gd–Cu coupling with $J_{Cu-Cu} = 9.9$ and $J_{Gd-Cu} = -0.15\,\text{cm}^{-1}$, with an averaged g value fixed at 2.00. The presence of the antiferromagnetic coupling was confirmed by the analysis of the magnetic behaviour of **7**,[11] a La^{III} derivative of **6**, where the magnetism depends only on the presence

$[Cu_2La_2(mhp)_4(OMe)_2(NO_3)_4(Hmhp)_2(MeOH)_4]$ **7**

of the two Cu^{II} ions. For **7** the magnetic susceptibility has a maximum value that is characteristic of an antiferromagnetic dimer. The experimental data for **7** were well reproduced by the Bleaney–Bowers equation[15] with $J_{Cu-Cu} = 14.6\,\text{cm}^{-1}$ and $g = 2.05$. The low-temperature behaviour of this complex can be modelled by assuming the presence of a 0.01 % amount of an $S = {}^1/_2$ paramagnetic impurity. For both **6** and **7** the magnitude of the antiferromagnetic J_{Cu-Cu} exchange is consistent with the well-known correlation[16] between this coupling and the Cu-O-Cu angle at the bridging O atoms, which in these molecules are 98.4(3) and 98.7(2)°, respectively.

The analysis of the magnetic behaviour of **2** was again based on the molecular structure. At first glance one might assume that the magnetism of this compound is determined by the central Gd–Cu interaction plus the contribution of two noninteracting copper ions, as the bridges connecting the inner part of the cluster to the two external Cu atoms (Cu 2 and Cu 3) are very long. With this simple model it was possible to simulate the high-temperature data down to the maximum observed in the χT curve at 22.5 K, but not the data below this temperature. As the decrease in the χT values could be due to saturation effects, we repeated the measurements with lower external magnetic fields. The data reported in Figure 3 were collected in a field of 0.05 T, and even here the low-temperature data are well below any values calculated for the model with one coupling constant.

We therefore examined several further Hamiltonians based on different coupling schemes. The one that yielded the best overall fit was based on the presence of one magnetic interaction between the central Gd 1 – Cu 1 pair and a secondary interaction between Gd 1 and the external Cu centres. To account for the possibility that Cu–Cu exchange pathways, due to an interaction through the diamagnetic bridges and through the gadolinium ion, are significant, two different Cu–Cu coupling constants ($J_{Cu1-Cu2}$ and $J_{Cu1-Cu3}$) were also introduced into the Hamiltonian. The best fit parameters obtained for **2** with a g value fixed at 2.00 were: $J_{Cu1-Cu2} = 8.20$, $J_{Cu1-Cu3} = 12.52$, $J_{Gd1-Cu1} = -3.51$, and $J_{Gd1-Cu2} = J_{Gd1-Cu3} = -0.11\,\text{cm}^{-1}$, with a calculated ground state with $S = 4$.

For the Gd_2Cu_4 cluster **5**, the spin Hamiltonian utilised assumes the presence of only one Cu–Cu exchange interaction and two different pairs of Gd–Cu interactions, as suggested by the observed crystal structure. The fitting procedure yielded : $J_{Cu-Cu} = 17.42$, $J_{Gd1-Cu1} = J_{Gd1-Cu2} = -2.84$ and $J_{Gd1-Cu1b} = J_{Gd1-Cu2b} = -0.55\,\text{cm}^{-1}$, with a fixed g value of 2.00. An alternative model in which four equivalent Gd–Cu interactions were used in the calculation led to the magnetism of the cluster being dominated by the frustration of the two gadolinium spins; this resulted in low-temperature behaviour in complete disagreement with that observed.

Conclusion

The results of the analysis of the magnetic data are in full agreement with the magnetic behaviour previously observed for Cu–Gd complexes.[1–6] For **2**, **5** and **6** the Gd–Cu interactions were found to be ferromagnetic in nature with magnitudes from -0.11 to $-3.51\,\text{cm}^{-1}$. In previous work the largest such coupling to be observed[1] was $-7.4\,\text{cm}^{-1}$. The mechanisms proposed to explain the ferromagnetic coupling[1, 5] envisage interaction between the ground state of the molecule and an excited state in which charge is transferred between the copper 3d orbitals and an orbital on gadolinium.[1, 5] Recent calculations of the energies of the allowed interactions between the ground configuration and the metal–metal charge-transfer configurations suggest that the mechanism involving a copper 3d orbital and a gadolinium 5d orbital is the most probable, and that the size of the coupling is consistent with the energy difference.[5] The question of which structural features influence the magnitude of the exchange coupling has not previously been discussed.

Although the number of complexes for which such coupling has been reported remains small, we decided to examine whether some form of magneto-structural correlation exists in this class of complexes. As the nature of the bridging unit is not the same for all reported complexes, varying from simple μ_2-oxygen atoms to extended bridging ligands such as oxamidato groups, we have restricted our attention to common features, namely, the Gd $\cdots$ Cu and Cu $\cdots$ Cu distances (if two or more Cu atoms are present).

It is immediately apparent that there is no correlation between Cu $\cdots$ Cu distance and the magnitude of the relevant coupling constant, however, the Gd $\cdots$ Cu distances (d_{Gd-Cu}) and the corresponding J_{Gd-Cu} exchange constant seem to be correlated by an exponential function of the type shown in Equation (1), where $A = 6.409 \times 10^4$ and $B = -2.833$. The relevant

$$-J_{Gd-Cu} = A\exp[B\,d_{Gd-Cu}] \tag{1}$$

values of J_{Gd-Cu} and d_{Gd-Cu} are listed in Table 4, and plotted in Figure 6. This is the first attempt to rationalise the magnetic behaviour of this type of system, and it is worth noting that the exponential correlation found may be related to the magnetic orbital overlap as suggested for other, unrelated exchange-coupled systems. The quality of fit and the limited number of experimental data mean that at this stage such a correlation must

Table 4. Gd – Cu coupling constants [a] and Gd – Cu distances in structurally characterised complexes.

	$-J_{Gd-Cu}$/ cm^{-1}	d_{GdCu}/Å	Ref.
$[\{Cu(hapen)_2\}_2Gd(H_2O)_3](ClO_4)_3$ [b]	5.3	3.367(5)	[1a]
$[\{Cu(SALen)\}_2Gd(H_2O)_3](ClO_4)_3$ [c]	7.4	3.30(1)	[1a]
$[\{Cu(SALtn)\}_2Gd(H_2O)(NO_3)_2]$ [d]	1.22	3.35(1)	[1b]
$[Gd(hfac)_3Cu(Satn)OH)]_2$ [e]	2.84	3.323(1) [f]	[3]
$[Gd_2\{Cu(pba)\}_3Cu(H_2O)_5]\cdot 20\,H_2O$ [g]	0.15	5.2799(4)	[6]
$[Gd_2Cu_4(fsaaep)_4(NO_3)_6]\cdot 0.5\,MeOH\cdot 0.5\,H_2O$ [h]	6.0	3.400(3) [i]	[5]
$[Gd\{Cu(BADPO)\}_2(H_2O)_4](NO_3)_3\cdot 2\,H_2O$ [j]	0.77	5.682(2)	[20]
$[Cu_2Gd_2(OMe)_2(mhp)_4(NO_3)_4(Hmhp)_2]$	0.15	4.285(1)	this work
$[Cu_3Gd(chp)_8(NO_3)(H_2O)]\cdot 0.5\,MeOH$	3.51	3.627(1)	this work
$[Cu_3Gd(chp)_8(NO_3)(H_2O)]\cdot 0.5\,MeOH$	0.11	3.833(1)	this work
$[Cu_4Gd_2Cl_4(hp)_8(Hhp)_4(H_2O)_2]\cdot 2\,Cl$	2.84	3.548(2)	this work
$[Cu_4Gd_2Cl_4(hp)_8(Hhp)_4(H_2O)_2]\cdot 2\,Cl$	0.55	4.333(2)	this work

[a] Negative sign indicates ferromagnetic coupling. [b] hapen = *N,N'*-ethylenebis(*o*-hydroxyacetophenoneiminato). [c] SALen = *N,N'*-ethylenebis(salicylaldiminato). [d] SALtn = *N,N'*-propane-1,3-diyl-bis(salicylaldiminato). [e] hfac = hexafluoroacetylacetonato; Satn = *N*-(3-aminopropyl)salicylaldiminato. [f] Distance reported is for isomorphous dysprosium complex. [g] pba = 1,3-propylenebis(oxamato). [h] fsaaep = 3-(*N*-2-(pyridylethyl)formimidolyl)salicylate. [i] Distance reported is for isomorphous praesodymium complex. [j] BADPO = *N,N'*-bis(3-amino-2,2-dimethylpropyl)oxamato.

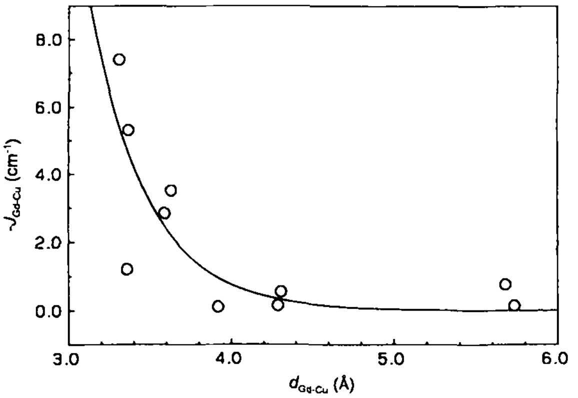

Fig. 6. A plot of $-J_{GdCu}$ against d_{GdCu} for all Gd – Cu complexes for which structural and magnetic data are available. The solid line represents A exp[d_{Gd-Cu} B] and shows the exponential relationship between J and d (see text for values of A and B).

remain merely a working hypothesis. Studies of further Cu – Gd complexes are now required to confirm or disprove this correlation.

Experimental Procedure

Compounds 1, 5 and 6 were prepared as described previously [4,9,11].

$[Cu_3Gd(chp)_8(NO_3)(OH_2)]$ (2): Complex **1** (5.2 mmol) was dissolved in CH_2Cl_2 (150 mL) to give a red solution. Hydrated gadolinium nitrate (0.9 mmol) dissolved in MeOH (15 mL) was added, and the solution turned green. The solution was filtered and evaporated to dryness, leaving a green tar. This was then redissolved in methanol (15 mL), the solution filtered and ether vapour allowed to diffuse into the filtrate. Dark green crystals grew over a period of one week; yield 20%. Elemental analysis: Found: C, 32.5; H, 2.2; N, 8.4. Calculated for **2**·MeOH: C, 33.0; H, 2.0, N, 8.5.

$[Cu_3Dy(chp)_8(NO_3)(OH_2)]$ (3) was synthesised in an identical manner to **2**; yield 28%. Elemental analysis: Found: C, 32.5; H, 2.2; N, 8.4. Calculated for **3**·MeOH: C, 33.0; H, 2.0, N, 8.5.

$[Cu_3Er(chp)_8(NO_3)(OH_2)_{0.5}(HOMe)_{0.5}]$ (4) was synthesised in an identical manner to **2**; yield 15%. Elemental analysis: Found: C, 32.5; H, 2.2; N, 8.6. Calculated for **6**: C, 32.7; H, 1.9, N, 8.6.

Crystallography: Crystal data and data collection and refinement parameters for compounds **2**–**4** are given in Table 1; selected bond lengths and angles for **2** in Tables 2 and 3, respectively.

Data collection and processing: Data were collected on a Stoë Stadi-4 four-circle diffractometer equipped with an Oxford Cryosystems low-temperature device [17] operating at 150 K, with graphite-monochromated $Mo_{K\alpha}$ radiation and $\omega-2\theta$ scans using the learnt-profile method [18]. Data were corrected for Lorentz and polarisation factors.

Structure analysis and refinement: All structures were solved by heavy-atom methods which revealed the position of the lanthanoid atom. All remaining non-hydrogen atoms were located from subsequent ΔF maps. In **2** and **3** all non-H atoms and in **4** Cu and Cl atoms were refined anisotropically. The hydrogen atoms were included in the refinements at idealised positions (C–H 1.08 Å), and with fixed isotropic thermal parameters [U = 0.05 Å^2]. Structure **4** displayed some disorder in the region of Cu2, where the site occupied by water in structures **2** and **3** was occupied 50% of the time by water and 50% by methanol. All calculations used SHELX76 [19] and published scattering factors [20].
Further details of the crystal structure investigations may be obtained from the Director of the Cambridge Crystallographic Data Centre, 12 Union Road, Cambridge CB2 1EZ, UK, on quoting the full journal citation.

Magnetic Studies: Magnetic susceptibility measurements were performed either on a DSM 5 magnetometer equipped with a Bruker BE-15 electromagnet and an Oxford Instruments CF 1200S continuous-flow cryostat or on an SHE superconducting SQUID susceptometer. Data were corrected for magnetisation of the sample holder and for diamagnetic contributions with Pascal's constants.

Acknowledgments: We thank the SERC for funding a studentship (to P. E. Y. M) and for funding for a diffractometer. We also thank the Leverhulme trust for a postdoctoral fellowship (to J. M. R).

Received: January 27, 1995 [F 74]

[1] a) A. Bencini, C. Benelli, A. Caneschi, R. L. Carlin, A. Dei, D. Gatteschi, *J. Am. Chem. Soc.* **1985**, *107*, 8128; b) A. Bencini, C. Benelli, A. Caneschi, A. Dei, D. Gatteschi, *Inorg. Chem.* **1986**, *25*, 572.
[2] N. Matsumato, M. Sakamoto, H. Tamaki, H. Okawa, S. Kida, *Chem. Lett.* **1989**, 853.
[3] C. Benelli, A. Caneschi, D. Gatteschi, O. Guillou, L. Pardi, *Inorg. Chem.* **1990**, *29*, 1751.
[4] A. J. Blake, P. E. Y. Milne, P. Thornton, R. E. P. Winpenny, *Angew. Chem. Int. Ed. Engl.* **1991**, *31*, 1139.
[5] M. Andruh, I. Ramade, E. Codjovi. O. Giullou, O. Kahn, J. C. Trombe, *J. Am. Chem. Soc.* **1993**, *115*, 1822 and references therein.
[6] O. Guillou, P. Bergerat, O. Kahn, E. Bakalbassis, K. Boubekeur, P. Batail, M. Guillot, *Inorg. Chem.* **1992**, *31*, 110.
[7] S. Wang, S. J. Trepanier, M. J. Wagner, *Inorg. Chem.* **1993**, *32*, 833.
[8] A. J. Blake, R. O. Gould, P. E. Y. Milne, R. E. P. Winpenny, *J. Chem. Soc. Chem. Commun.* **1991**, 1453.
[9] A. J. Blake, R. O. Gould, P. E. Y. Milne, R. E. P. Winpenny, *J. Chem. Soc. Chem. Commun.* **1992**, 522,
[10] A. J. Blake, P. E. Y. Milne, R. E. P. Winpenny, *J. Chem. Soc. Dalton Trans.* **1993**, 3727.
[11] A. J. Blake, V. A. Cherepanov, A. A. Dunlop, C. M. Grant, P. E. Y. Milne, J. M. Rawson, R. E. P. Winpenny, *J. Chem. Soc. Dalton Trans.* **1994**, 2719.
[12] For example, K. K. Bhandary, H. Marokar, *Acta. Crystallogr. Sect. B.* **1976**, *32*, 861.
[13] D. Gatteschi, L. Pardi, *Gazz. Chim. Ital.* **1993**, *123*, 21.
[14] F. James, M. Roos, *Comput. Phys. Commun.* **1975**, *10*, 343.
[15] B. Bleaney, K. D. Bowers, *Proc. R. Soc. London Ser. A* **1952**, *214*, 451.
[16] W. E. Hatfield in *Magneto-Structural Correlations in Exchange Coupled Systems* (Ed.: R. D. Willett, D. Gatteschi, O. Kahn), *NATO ASI Ser. Ser. C*, **1985**, *140*, 555.
[17] J. Cosier, A. M. Glazer, *J. Appl. Crystallogr.* **1986**, *19*, 105.
[18] W. Clegg, *Acta Crystallogr. Sect. A*, **1981**, *37*, 22.
[19] G. M. Sheldrick, SHELX76, Program for crystal structure refinement, University of Cambridge, 1976.
[20] *International Tables for X-ray Crystallography*, Kynoch, Birmingham, **1974**, vol. 4, pp. 19–149.